Measurement Of Heavy Vehicle Dynamic Wheel Forces Using A Bolt-On Transducer

Wu-Shan Yang, Chandrashekhar Doedhar, Donald A. Streit, and Bohdan T. Kulakowski
The Pennsylvania State University, USA

ABSTRACT

A new wheel force transducer has been designed, fabricated and tested. The transducer design is first described. Algorithms used to process transducer signals are then discussed. Finally, system testing results are shown to have good correlation with axle strain data.

INTRODUCTION

There has been a continual search for means to measure dynamic tire forces on pavement. Particularly when dealing with heavy vehicles, the interest is to identify a tool which is useful in studying both the effect of vehicle dynamics on dynamic pavement forces, and also the effect of road profile on vehicle response. It is reasonable to expect that the closer the measurement is made to the point of interest (at the tire/pavement contact patch), the better will be the measurement. Ideally, an instrument would be mounted to the surface of the tire and, as the vehicle traveled, the instrument would report the dynamic forces between the tire and the road. Because an instrument such as this does not exist, other measurement locations have been considered. For example, one standard approach is to mount strain gages on the axles of vehicles to determine dynamic axle loads. By estimating the mass outboard from the strain gage location and using accelerometer data, inertial loading can be approximately determined and dynamic wheel loads on pavement can be back calculated. Several difficulties exist with this approach. First, it is very difficult to accurately estimate the mass which is outboard from the axle strain gage. Accurate determination of this parameter can require disassembly of the axle. Second, depending on the configuration of an axle and suspension, it is often difficult to mount gages in appropriate locations on the axle housing.

To address these difficulties, a new wheel force transducer (WFT) has been designed. The transducer mounts between a wheel and a hub. In the following sections, design criteria is first presented. The WFT design which meets these criteria is then described. System mounting and operations are discussed, and WFT performance is compared against axle strain gage data.

WFT DESIGN REQUIREMENTS

WFT design criteria include the following.

1. Weight should be kept below 100 lbf. Simulations shown that if weight is kept below 300 lbf, dynamic wheel forces will change by less than 5%
2. System stresses must be low enough to provide fatigue life of better than 1e6 cycles. This is often correlated with infinite life when considering fatigue loading of steel.
3. Vertical and forward/backward horizontal wheel forces should be measured.
4. Wheel offset should be minimum.
5. The WFT should be mountable to a heavy vehicle without making any modifications to the vehicle or wheel.
6. The transducer and wheel should be mountable using standard impact wrench and socket.
7. Standard wheel bolt torque specifications should be achievable for mounting of both the transducer and the wheel.
8. On-wheel electronics must be rugged enough to withstand operating conditions.
9. Slip rings should not corrupt strain gage data.
10. The WFT and electronics housing should be easily transportable.
11. The WFT should be able to be conveniently mounted and dismounted by one person.

12. Acceleration must be measured to allow inertial correction to WFT measurements.

13. Wheel orientation must be measured to within 0.5° accuracy.

These items are here briefly considered.

WFT DESIGN

WFT force ring schematics are given in Figures 1, 2, and 3. Only nominal dimensions are shown in these figures.

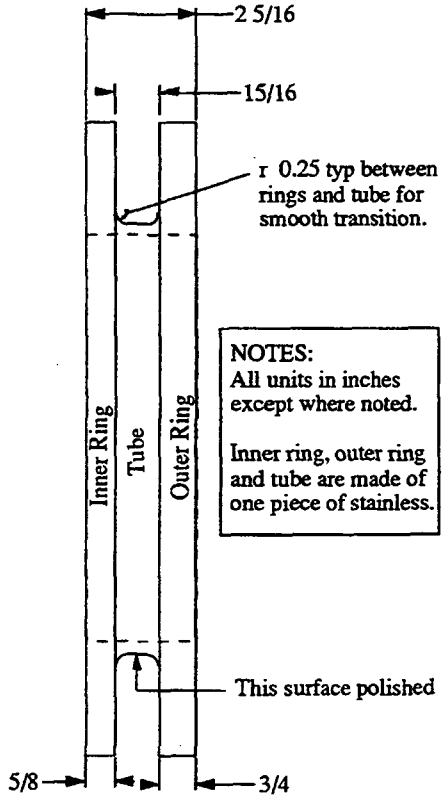

Figure 1. Edge view of WFT strain gaged force ring

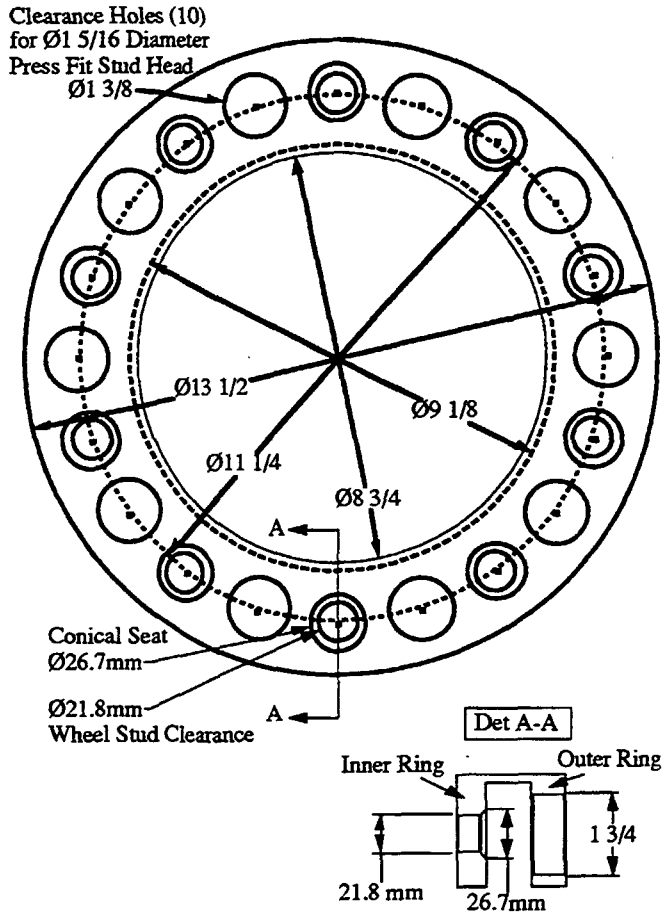

Figure 2. WFT inside ring.

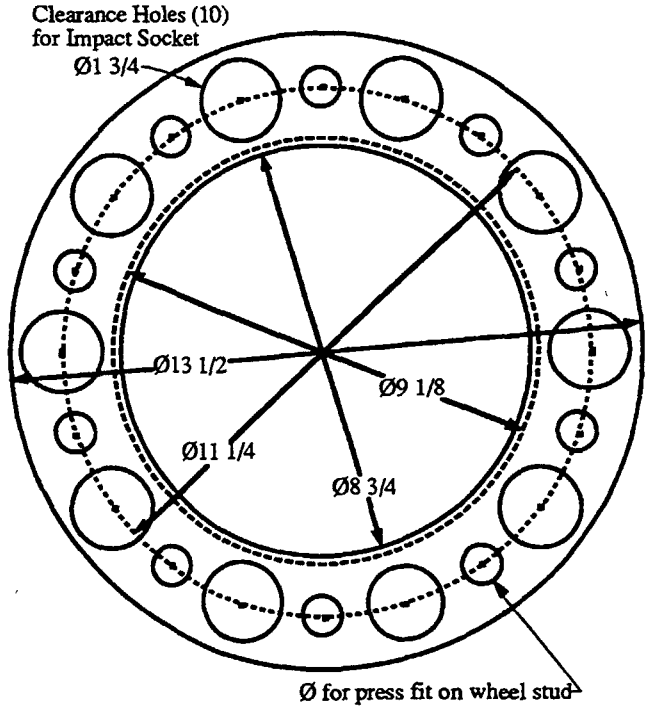

Figure 3. WFT outside ring.

The overall width of the force ring was determined by both ring thickness and tube length requirements. A FEM of this strain gaged force ring was performed to identify stress concentrators which might arise from holes in the inner ring, holes in the outer ring, tube thickness, or tube-to-ring radius. The tube length of 15/16 inches provided a uniform strain field which responded linearly to applied loads.

The inside ring is designed to slide over the studs of standard Budd wheels. The inner ring is secured to the hub using inner nut cups. Because the square head of an inner nut is relatively small, a stock impact socket is available with an outside diameter which will fit through the 1 3/4 inch clearance hole in the outside ring. Inner/outer ring hole alignment for inner nut cup fastening is given as detail A-A in Figure 2. This arrangement allows use of standard pneumatic tools for WFT mounting and dismounting.

Studs are attached to the outside ring of the WFT to allow mounting of a wheel. In order to provide enough strength to withstand the 750 ft-lbf bolt torque mounting specifications, the studs had to be press fit into the outer ring. This required clearance holes in the inner ring through which the studs were pressed. Single or dual Budd wheels can be mounted to the WFT in the usual manner.

Two full strain gage bridges are mounted onto the tube which is shown in the Figure 1 schematic. The bridges are 90° apart and are mounted such that strain arising from axial, torsional and bending wheel loads is canceled out. The strain gage bridges measure shear force only. Shear force is generated by either vertical wheel forces or by fore/aft horizontal wheel forces.

WFT ELECTRONICS

After the wheels are mounted to the WFT, an electronics housing is mounted to the outside wheel. Strain gage bridge wiring is brought into this housing for signal conditioning. Because voltage signals can be effected when passing through slip rings, strain gage amplifiers which provide current output were chosen. After bringing these signals through the slip rings, voltage across a precision resistor is monitored. The voltage signals are brought through a low pass anti-aliasing filter.

A resolver is also mounted in the electronics housing and an accelerometer is mounted on the non-rotating portion of the WFT. The resolver provides angular position resolution to 0.1°. All data are collected using a personal computer through an analog to digital converter board at a sampling rate of 200 Hz.

AXLE STRAIN MEASUREMENTS

In order to compare WFT performance in the field, strain gages were mounted to the rear axle of a truck. Shear gages were mounted to the front and back sides of the axle housing.

TEST PROCEDURE

The wheel force transducer is mounted on a vehicle. The static wheel load is measured using a wheel scale. Care is taken to when measuring the static wheel load so that the truck remains horizontal. This is accomplished using wooden blocks under the other wheels with height equal to the wheel scale height. The vehicle is driven slowly on a level surface. When the clutch is free and the vehicle is slowly coasting, horizontal forces are minimum and dynamic vehicle oscillations are relatively small. WFT data is collected. This data is used to identify a zero angle reference position, and also to generate error correction data to be applied to high speed tests.

WFT ALGORITHMS

Vertical force Fv and horizontal force Fh on the wheel force transducer can be calculated as follows.

$$Fv = Fa \sin\theta + Fb \cos\theta \quad (1)$$
$$Fh = Fa \cos\theta - Fb \sin\theta \quad (2)$$

where

$Fa = Ca * Va + Cao$
$Fb = Cb * Vb + Cbo$

and

Ca, Cao - calibration factor slope and offset for strain gage bridge 'a'.
Cb, Cbo - calibration factor slope and offset for strain gage bridge 'b'.
Va - bridge 'a' output voltage
Vb - bridge 'b' output voltage
θ - wheel angle given by resolver

The total dynamic forces at the interface between the tire and the road can be calculated using (1) and (2) with inertial force compensation. Then the vertical and horizontal forces at the tire/pavement contact, Fvw and Fhw, respectively are given by Whittemore et al. [1970] and LeBlanc et al. [1992] to be

$$Fvw = Fv + W + Fvi \quad (3)$$
$$Fhw = Fh + Fhi \quad (4)$$

where

$Fvi = \sum M * Avi$
$Fhi = \sum M * Ahi$

and

W - static wheel and tire weight
Fvi - all vertical inertial forces due to mass outboard from the WFT
Fhi - all vertical inertial forces due to mass outboard from the WFT
M - mass outboard from WFT
Avi - vertical acceleration of center of gravity of wheel(s)
Ahi - horizontal acceleration of center of gravity of wheel(s)

DATA PROCESSING

If the WFT were a perfect measurement instrument, and if the vehicle were rolling on a flat, horizontal surface, and if the vehicle were not vibrating or bouncing at all, then the output for bridge 'a' and bridge 'b' would be a perfect sine and cosine wave, respectively, for one wheel rotation. Since this is not the case, error will be observed in the WFT signals. It is very helpful to recognize that the predominant error in this instrument is periodic in one wheel rotation $\theta = 0$ to 360°. This is true for any imperfection in WFT material homogeneity, strain gage mounting and strain gage bridge response. The convenience that this inherent factor provides is that the Fourier transform is ideally suited to provide an error correction algorithm for the WFT. The error correction will be explained in terms of the bridge 'a' and bridge 'b' voltage reported in Figures 4 and 5.

The data of figures 4 and 5 were obtained by successively incrementing the truck forward by approximately 30° of wheel rotation for slightly more than one complete wheel revolution. At each wheel rotation increment, the vehicle is stationary and, without any applied brake force, WFT data is collected from both strain gage bridges 'a' and 'b'. The bridge data which is collected is purely static data arising from vertical wheel loads, with negligible horizontal forces applied. 15 data points are reported in figures 4 and 5. From these figures, it can be observed that bridge 'a' produces a signal which is close to the expected sine wave, but bridge 'b' response deviates noticeably from the expected cosine wave.

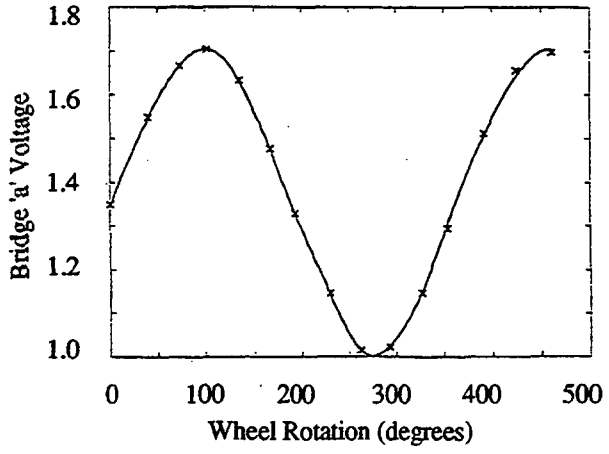

Figure 4. Bridge 'a' calibration data and 15 term Fourier series expansion.

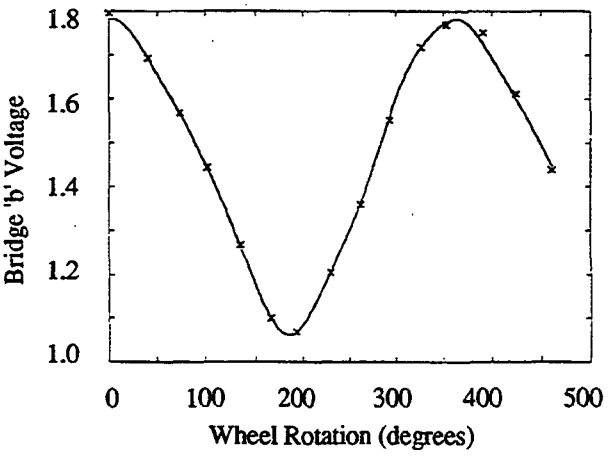

Figure 5. Bridge 'b' calibration data and 15 term Fourier series expansion.

The data from this static testing is not equally spaced. In order to generate equally spaced data for Fourier transform algorithms, a cubic spline curve fitting algorithm is applied to the 15 experimental points shown in Figures 4 and 5. Equally spaced data in θ is then obtained from these cubic curves and a 15 term Fourier series expansion of each of these curves is generated. The Fourier Series expansion of a periodic signal is given by:

$$V(\theta) = C_0 \cos \phi_0 + C_1 \cos(\theta + \phi_1) + C_2 \cos(2\theta + \phi_2) + C_3 \cos(3\theta + \phi_3) + \ldots \quad (5)$$

or,

$$V(\theta) = C_0 \cos \phi_0 + C_1 (\cos \phi_1 \cos \theta - \sin \phi_1 \sin \theta) + C_2 \cos(2\theta + \phi_2) + C_3 \cos(3\theta + \phi_3) + \ldots \quad (6)$$

Theoretically, in the perfect WFT, bridge 'a' should be a sine wave. Therefore, for static measurements, the error in bridge 'a' measurement is known to be the difference between the actual bridge 'a' response, and a perfect sine wave. If bridge 'a' responded perfectly as a sine wave, then $V(\theta)$ in (5) would equal $C_1 \sin\theta$. Therefore, all terms in (5) besides $C_1 \sin \theta$ can be considered error. V_a can therefore be corrected by:

$$V_{anew}(\theta) = [-V_a(\theta) + C_{a0} \cos \phi_{a0} + C_{a1} \cos \phi_{a1} \cos \theta + C_{a2} \cos(2\theta + \phi_{a2}) + C_{a3} \cos(3\theta + \phi_{a3}) + \ldots]/\sin \phi_{a1} \quad (7)$$

Similarly, if bridge 'b' responded perfectly as a cosine wave, then $V(\theta)$ in (5) would equal $C_1 \cos\theta$. Therefore, all terms in (5) besides $C_1 \cos \theta$ can be considered error. V_b can therefore be corrected by:

$$V_{bnew}(\theta) = [V_b(\theta) - C_{b0} \cos \phi_{b0} + C_{B1} \sin \phi_{b1} \sin \theta - C_{b2} \cos(2\theta + \phi_{b2}) - C_{b3} \cos(3\theta + \phi_{b3}) - \ldots]/\cos \phi_{b1} \quad (8)$$

It should be noted that the corrections of (7) and (8) shift the bridge 'a' and bridge 'b' voltage signals through

phase angles ϕ_{a1} and ϕ_{b1} respectively. These phase angles arise because some wheel position was assigned the θ=0°. However, when bridges 'a' and 'b' are combined to get vertical wheel force, an arbitrary choice of θ=0° will result in degradation of measurement accuracy. Bridge 'a' and 'b' maximum sensitivity will occur when the respective bridge is in its horizontal position. However, an arbitrary θ=0° position forces a less sensitive bridge position to provide a peak V_{anew} and V_{bnew} signal. To avoid this undesirable consequence, the θ=0° wheel orientation is carefully chosen. For perfect bridge 'a' and bridge 'b' response, then θ=0° when bridge 'b' (cosine) is maximum and θ=90° when bridge 'a' (sine) response is maximum. Because bridge 'a' and 'b' peaks are not 90° apart, an averaged value of θ corresponding to peak response of bridges 'a' and 'b' is used as follows:

$$\theta_0 = \theta(V_{bmax}) + \{90° - [\theta(V_{amax}) - \theta(V_{bmax})]\}/2 \quad (9)$$

where $\theta(V_{amax})$ corresponds to the value of θ when V is maximum for bridge 'a' in (7) and $\theta(V_{bmax})$ corresponds to the value of θ when V is maximum for bridge 'b' in (8). The values of ϕ_{a1} and ϕ_{b1} angles in (7) and (8) should be reasonably close to the value of θ corresponding to maximum bridge 'a' and 'b' voltages, respectively The value of θ_0 in (9) is then taken as the zero wheel orientation and V_{anew} and V_{bnew} are obtained from (7) and (8).

WFT PERFORMANCE

Calibration data has been collected and error correction applied to slow rolling vehicle tests. After inertial correction for both WFT and axle housing strain gage data, vertical wheel force is calculated and both signals are plotted in Figure 6. WFT response is shown to correlate very nicely with axle strain data. Force peaks between the two curves typically differ by less than 500 lbf or about 7% of the nominal signal.

Higher speed test data is shown in Figure 7. At 35 mph, peak forces reported by WFT and axle strain both indicate that similar vehicle dynamics is being captured.

CONCLUSIONS

A new wheel force transducer has been designed, fabricated and tested. Unique error correction algorithms have been derived and applied to accommodate the periodic irregularities which appear in the WFT strain gage bridge signals. The WFT response is shown to correlate well with axle strain data. The new Federal Highway Association Wheel Force Transducer provides a valuable research tool for studying both the effects of various vehicle configurations on pavement, and also the effects of various road profiles and pavement types on vehicles.

ACKNOWLEDGMENTS

The work reported in this paper was conducted under the sponsorship of the Federal Highway Administration. However, the findings and conclusions in the paper are those of the authors and do not necessarily represent the views of the Federal Highway Administration.

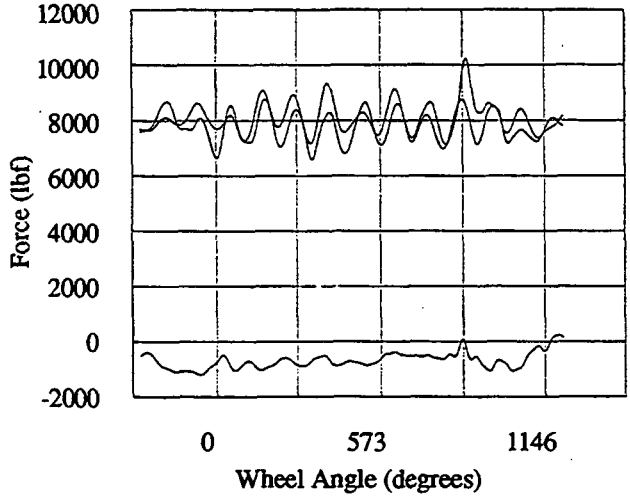

Figure 6. WFT and axle force measurements compared. Static wheel load = 7750 lbf, slow rolling.

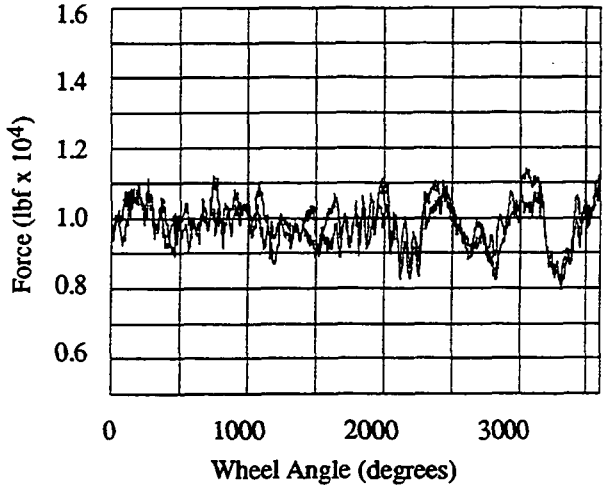

Figure 7. WFT and axle force measurements compared. Static wheel load = 10,490 lbf, 35 mph.

REFERENCES

LeBlanc, P. A., Woodrooffe, J. H. F., and A. T. Papagiannakis, A. T., "A comparison of the accuracy of two types of instrumentation for measuring vertical wheel load," Heavy vehicles and roads: technology, safety and policy, Thomas Telford, London, 1992.

Woodrooffe, J. H. F., LeBlanc, P. A., and K. R. LePiane, "Effects of Suspension Variations on the Dynamic Wheel Loads of a Heavy Articulated Highway Vehicle," Technical Report, Vehicle Weights and Dimensions Study, Volume 11, Roads and Transportation Association of Canada (RTAC), 1986.